Indonesian Physical Review

Volume 08 Issue 01, January 2025

P-ISSN: 2615-1278, E-ISSN: 2614-7904

Comparative Behavior of Magnetic Iron Oxide Nanoparticles (MIONs) via Mechanical and Chemical Routes

Ilham Dias Fajariman [1], Arif Hidayat [1], Markus Diantoro [1,2], Yoyok Adi Setio Laksono [1], Nurul Putri Wulandari [1], Nadiya Miftachul Chusna [3], Futri Yuliana [3], Kormil Saputra [3,4], and Sunaryono Sunaryono[1,2*]

[1] *Department of Physics, Faculty of Mathematics and Natural Sciences, Universitas Negeri Malang, Indonesia*

[2] *PUI-PT Centre of Advanced Materials for Renewable Energy, Universitas Negeri Malang, Indonesia*

[3] *Mions Laboratory, PT Cakra Mions Teknologi (Persero), Malang, Indonesia*

[4] *Physics Study Program, Faculty of Mathematics and Natural Sciences, University of Mataram, Indonesia.*

Corresponding Authors E-mail: sunaryono.fmipa@um.ac.id

Article Info

Article info:

Received: 26-09-2024

Revised: 05-12-2024

Accepted: 13-12-2024

Keywords:

Magnetic Iron Oxide; Nanoparticles (MIONs); Superparamagnetic; Mechanical Synthesis; Chemical Synthesis

How To Cite:

I. D. Fajariman, A. Hidayat. M. Diantoro, Y. A. S. Laksono, N. P. Wulandari, N. M. Chusna, F. Yuliana, K. Saputra, and Sunaryono, "Comparative behavior of magnetic iron oxide nanoparticles (MIONs) via mechanical and chemical routes", Indonesian Physical Review, vol. 8, no. 1, p 181-195, 2025.

DOI:

https://doi.org/10.29303/ipr.v8i1.407.

Abstract

This study successfully synthesized Magnetic Iron Oxide Nanoparticles (MIONs) through two different processes, namely mechanical synthesis (MIONs – M) and chemical synthesis (MIONs – N). The synthesized samples were characterized using X-Ray Fluorescence (XRF), Scanning Electron Microscopy (SEM), X-ray Diffraction (XRD), and Vibrating Sample Magnetometer (VSM) to determine the elemental composition, morphology, structure, and magnetization of the samples. XRF analysis revealed that iron (Fe) dominated both samples, with concentrations reaching 93.91% for MIONs – M and 89.91% for MIONs – N. SEM morphological analysis showed that the MIONs tended to be spherical and experienced agglomeration, with particle size distribution around 120 nm for MIONs – M and 30 nm for MIONs – N. XRD data indicated that both samples exhibited a cubic spinel Fe_3O_4 phase, consistent with the AMCSD 0000945 model data. Using the refinement method and Debye-Scherrer equation, the crystallite size and density of MIONs – M were found to be larger than MIONs – N. This correlates with VSM data analysis, where the saturation magnetization of MIONs – M (49.51 emu/g) was greater than that of MIONs – N (26.54 emu/g). These results provide important insights into the characteristics of MIONs and their implications for technological and industrial applications.

Introduction

The study of nanomaterial characteristics has seen rapid advancements in the fields of science and technology [1]. Nanoparticles offer numerous advantages over microparticles or bulk materials [2]. Specifically, the properties of nanoparticles are more pronounced than those of microparticles [3, 4], and their flexibility makes them suitable for current technological and industrial applications. This technological development allows materials to be conjugated with various additional molecules, creating new systems with enhanced and innovative specifications [5]. One material that is currently widely researched and developed for various applications is Magnetic Iron Oxide Nanoparticles (MIONs), particularly Fe_3O_4 (magnetite) nanoparticles [6-8].

Fe_3O_4 nanoparticles are of great interest due to their unique properties and potential applications in various fields. For example, in medicine, Fe_3O_4 nanoparticles are used as drug delivery agents by utilizing magnetic microgels [9], immunotherapy for treating murine mammary adenocarcinoma (breast cancer), as contrast agents for MRI, and in hyperthermia cancer treatment, combined with microorganisms using a bio-physical approach [10]. In industry, Fe_3O_4 can be applied as an adsorbent for removing malachite green from aqueous solutions [11], improving the durability of electrodes in lithium batteries, as supercapacitors for energy storage, and as sensitive electrochemical sensors for the simultaneous detection of dopamine, ascorbic acid, and uric acid [12].

The properties of Fe_3O_4 nanoparticles have become a topic of discussion due to their potential applications in fields such as environmental engineering, biomedicine, microfluidics, and electric field mechanics [2,13]. This is because Fe_3O_4 nanoparticles exhibit unique magnetic properties compared to their bulk counterparts. Under high-temperature treatment, ferromagnetic particles exhibit superparamagnetic behavior at specific crystal sizes, typically below ~10^{-8} m [14], [15]. Additionally, the magnetic spin, size, and morphology of Fe_3O_4 nanoparticles contribute to their magnetic properties, especially as superparamagnetic materials.

Fe_3O_4-based superparamagnetic materials are highly intriguing to explore, particularly in terms of their synthesis process. Research by Taufiq et al. [6] revealed that it is possible to synthesize Fe_3O_4 nanoparticles in the size range of 30–100 nm by varying the amount of ferric chloride and solvent. This approach promotes efficient adsorption of impurities in water and magnetic flocculation. The results demonstrated that the synthesized Fe_3O_4 nanoparticles exhibited superior magnetic performance compared to commercial Fe_3O_4 nanoparticles (100 nm), enabling effective recovery and separation of the magnetic flocculant. The removal rates for COD, ammonia nitrogen, and total phosphorus were found to be 93.48%, 100%, and 84.62%, respectively, after 7 days, with a magnetic flocculant recovery rate of 95%. However, the study did not thoroughly evaluate the impact of size variation on other functional properties, such as thermal stability or biocompatibility, which are critical for further applications. Although the magnetic performance is reported to be better than that of commercial Fe_3O_4, there is no detailed quantitative measurement, such as magnetization saturation (Ms), coercivity (Hc), or remanence (Mr), to provide a more objective comparison of performance. This study focuses on the characteristics of MIONs synthesized through different processes, namely mechanical preparation and chemical synthesis. Mechanochemical preparation involves the use of a planetary ball mill, while chemical synthesis is performed via the coprecipitation method. The coprecipitation method is a synthesis technique that

involves the simultaneous precipitation of iron precursors in solution to produce Fe_3O_4 nanoparticles. This process entails the reaction of iron salt solutions with a base under specific temperature conditions to form magnetite nanoparticles [15-17]. The coprecipitation method offers advantages such as precise control over particle size and the ability to produce nanoparticles with desired magnetic properties.

Experimental Method

A. Material

The basic materials used in this study were iron sand from Sine Beach, Tulungagung, East Java. Other synthetic materials were hydrochloric acid (HCl) 37% Merck, ammonia hydroxide 25% (NH_4OH) Merck, distilled water, DI Water, and alcohol. While the tools used included permanent magnets, hot plate magnetic stirrer, digital scales, stopwatches, 100 ml measuring cups, 100 ml beakers, 250 ml beakers, spatulas, filter paper, tissues, funnels, droppers, marble mortars, tweezers, pH paper, petri dishes and ovens.

B. Mechanochemical Preparation for MIONs - M

The mechanochemical preparation process for MIONs – M begins with the separation of iron sand using a magnet to isolate iron-rich material from non-magnetic impurities. The separated material is then washed with deionized water and a dilute HCl solution to remove impurities and enhance purity, followed by rinsing with deionized water until the pH of the rinsing solution reaches 7. The material is then dried at 100 °C. Subsequently, the material is reduced to nanoscale dimensions through ball milling for 12 hours at a rotational speed of 500 rpm, ensuring homogeneity and increased surface area. Finally, the material is heated in a furnace at 300–500°C for 4 hours to crystallize magnetic phases such as MIONs -M. The mechanochemical preparation process for MIONs – M is illustrated in **Figure 1**.

Figure 1. Illustration of mechanochemical preparation of MIONs–M Samples

C. Synthesis of MIONs-N with coprecipitation method

For the preparation of the MIONs–N sample, the synthesis process also began by washing the iron sand with distilled water and drying it under sunlight until fully dry. The iron sand was then separating the iron sand using a permanent magnet to isolate iron sand from non-magnetic impurities. The next step involved reacting 20 g of iron sand powder with 58 ml of HCl solution using a magnetic stirrer hotplate at room temperature with a stirring speed of 720 rpm for 30 minutes. Once the solution was homogeneously mixed, it was filtered to obtain a solution containing Ferrous Chloride ($FeCl_2$) and Ferric Chloride ($FeCl_3$). A total of 18 ml of $FeCl_2$ and $FeCl_3$ solution was then titrated with 25 ml of NH_4OH solution and stirred on a magnetic stirrer hotplate at a speed of 720 rpm for 30 minutes. The titration product was then

washed with DI water until neutral pH (pH 7) was achieved. The synthesis process continued by filtering the washing product to obtain Fe_3O_4 nanoparticles. In the final step, the Fe_3O_4 nanoparticles were oven-dried at 100°C for 1 hour to obtain the MIONs–N sample. The synthesis process for MIONs–N is illustrated in **Figure 2**.

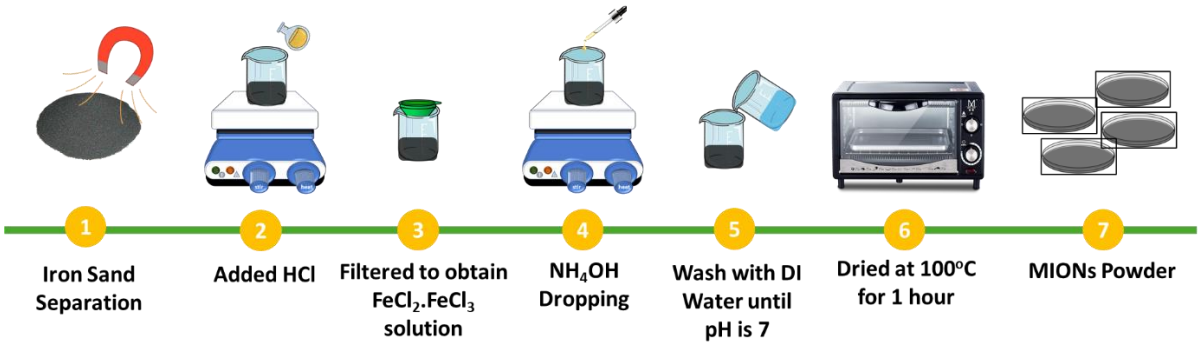

Figure 2. Illustration of Chemical Synthesis of MIONs–N Samples

C. Sample Characterization

The characterization of MIONs–M and MIONs–N samples was performed using several advanced instruments. X-ray diffraction (XRD) analysis was conducted with an X'Pert3 Powder (PANalytical Company B.V., Netherlands) over a 2θ range of 11° to 90°. This characterization aimed to study the formed magnetite phase, particle size, and lattice parameters based on the AMCSD 005203 model data. The proportion of the phases formed was analyzed using the Rietveld method, assisted by Rietica software. Scanning Electron Microscopy (SEM) (FEI, Type: Inspect-S50, China) was employed to investigate the morphology of the MIONs–M and MIONs–N samples. X-ray fluorescence (XRF) (PANalytical, Type: Minipal 4, UK) was used to determine the elemental composition of the iron sand. Meanwhile, magnetization, coercivity, and susceptibility tests were conducted using a Vibrating Sample Magnetometer (VSM) with the Physical Properties Measurement System (PPMS) Quantum Design PPMS® VersaLab™ Cryogen-free 3 Tesla, USA.

Result and Discussion

The MIONs–M and MIONs–N samples are samples resulting from different syntheses, where the MIONs–M sample is a sample synthesized by mechanical methods while the MIONs–N sample is the result of chemical synthesis. Both samples were characterized using an XRF instrument to determine the elemental composition of each sample. This is important to do to determine the composition contained in the sample. Different elemental contents can affect the magnetic performance, stability, and usability of the sample material. The complete XRF characterization results of the samples are shown in Figure 2.

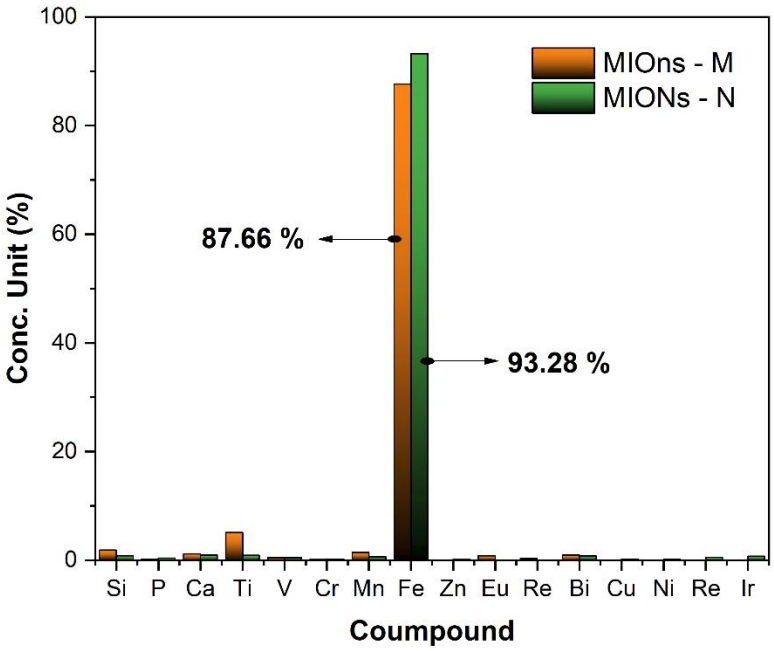

Figure 2. Element content of MIONs – M and MIONs – N samples

Figure 2 shows the elemental composition of the MIONs – M and MIONs – N samples. The percentage of iron (Fe) dominates both samples, followed by titanium (Ti), and calcium (Ca), as well as other minor elements. The elemental content in the MIONs – M and MIONs – N samples can be compared with several previous research reports. The results of the data comparison show that the Fe element content is generally relatively similar to the results of another research. Details of the elemental comparison can be seen in Table 1.

Table 1. MIONs Compound Compare in Another Research

Compound	Percentage (%)				
	MIONs – M	**MIONs – N**	**Ref.** [17]	**Ref.** [19]	**Ref.** [20]
Si	1.83	0.8	0.82	0.80	0.84
P	0.2	0.4	0.21	1.35	0.18
Ca	1.17	0.94	0.15	0.92	0.16
Ti	5.07	0.87	5.80	7.20	5.85
V	0.44	0.42	0.45	0.40	0.46
Cr	0.12	0.24	0.11	0.14	0.13
Mn	1.45	0.66	0.43	0.60	0.47
Fe	87.66	93.28	89.80	86.10	90.00
Zn	0.04	0.1	0.05	0.11	0.04
Eu	0.79	--	0.80	-	0.78
Re	0.3	--	0.28	-	0.32
Bi	0.93	0.77	0.94	0.76	0.95
Cu	--	0.15	-	0.12	-
Ni	--	0.15	-	0.15	-
Re	--	0.5	-	0.72	-
Ir	--	0.72	-	-	-

Table 1 shows the elemental composition of the MIONs – M and MIONs – N samples. In general, the elemental composition contained in both samples is consistent with several existing references. The results of data analysis show that the iron (Fe) element content is more dominant than other elements for both samples, where the MIONs – M sample contains 86.00% and MIONs – N is 89.91% Fe. The Fe element content of the MIONs – N sample is in accordance with previous research which showed a value of 90% [21]. This shows that the MIONs – N sample with the coprecipitation synthesis method has optimum purity than the mechanical method.

The purity of the sample elements plays an important role in optimizing the mechanical and magnetic properties of the sample. In addition to the Fe element, the titanium (Ti) element is in the second highest position of the two samples. The Ti element content reaches 5.07% for the MIONs – N sample. This Ti element content is in accordance with the reference, which is around 0 to 5.80%. The high Ti in this case is due to the calcination effect which still leaves impurities.

Manganese (Mn) is one of the elements contained in the MIONs – N and MIONs – M samples, each at 0.66% and 1.45%. This percentage is in line with reference data from previous research. The content of other elements such as silicon (Si), phosphorus (P), and calcium (Ca) also show different values. MIONs – M has a Si content of 1.83% while MIONs – N is 0.8%. This value is close to the reference data which shows a value of 0.80% to 0.84% [16]. In contrast to the Si element, the phosphorus element shows a significant difference between the two samples, where the MIONs – N sample has a content of 0.20% while the MIONs – M sample is 0.40%. This difference is due to the behavior of element breakdown in the synthesis process or raw materials. The same thing was also detected in the element Calcium (Ca) where the MIONs - M sample contains less Ca, which is 1.17% compared to the MIONs - N sample which is in the range of 0.94%. Other elements such as vanadium (V), chromium (Cr), and zinc (Zn) show good consistency between the two samples and the reference, with element contents close to the data in the literature. It is also interesting to find the elements europium (Eu) and rhenium (Re) only in the MIONs - M sample and the elements copper (Cu), nickel (Ni), rhenium (Re), and iridium (Ir) only in the MIONs - N sample.

These results indicate that the composition of these elements may not be uniform or only exist under certain conditions [22]. The morphology of the MIONs - M and MIONs - N samples was successfully characterized using an SEM instrument as shown in **Figure 3**. The characterization of both samples was carried out at two different magnifications, namely magnification with a scale bar of 100 μm and 2 μm. The difference in scale bars aims to see the surface characteristics of the two MIONs samples. At a scale bar magnification of 100 μm, the surface characteristics of the two MIONs samples were not detected well and tended to be random. In contrast to the scale bar magnification of 2 μm, the characteristics of the two MIONs samples were spherical and appeared to experience agglomeration between one particle and another. These results are well confirmed by previous studies which stated that magnetite has a spherical shape [23]. In addition, both MIONs samples were spread into several clusters which means that magnetite tends to experience agglomeration as a result of the electromagnetic properties of the two samples, namely the attractive force between the magnetic dipoles of magnetite particles. These results are also in line with previous research reports which explain that magnetite particles in nano sizes have strong properties to experience agglomeration [8].

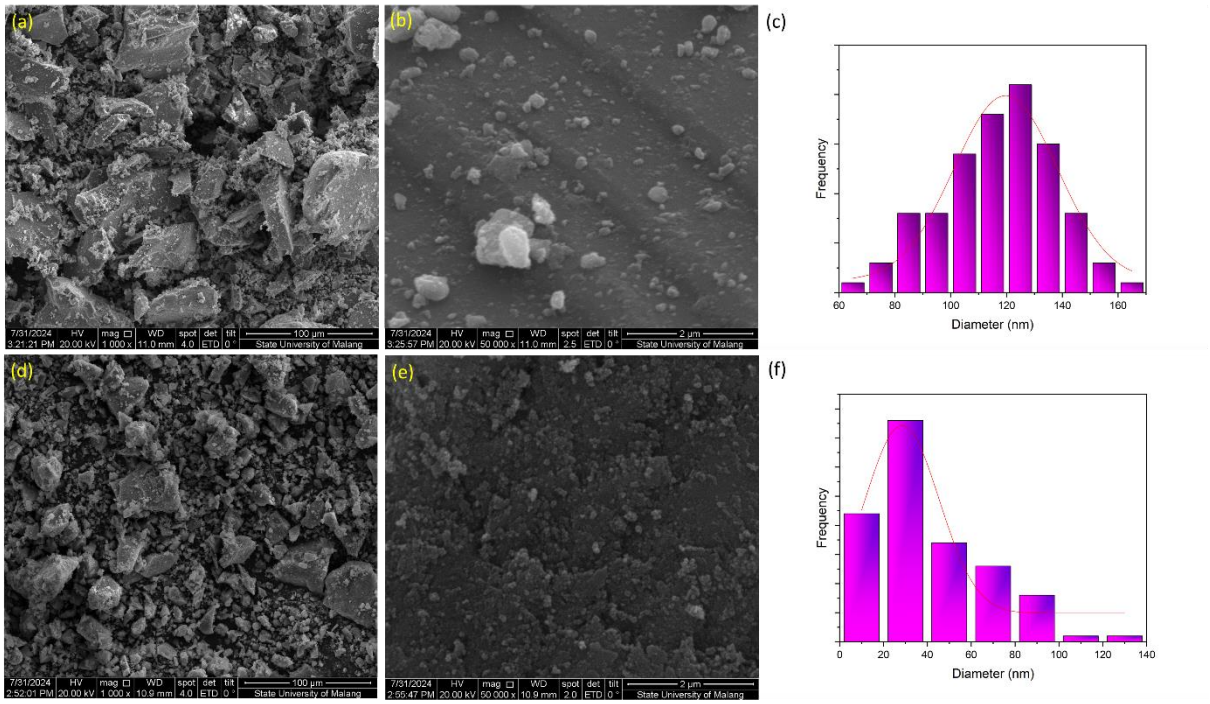

Figure 3. Morphology of samples (a) MIONs – M with a scale bar of 100 µm, (b) MIONs – M with a scale bar of 2 µm, (c) Particle size distribution of MIONs – M, (d) MIONs – N with a scale bar of 100 µm, (e) MIONs – N with a scale bar of 2 µm, (f) Particle size distribution of MIONs – N

Figure 3 also shows the particle size distribution of both MIONs samples. The results of data analysis show that the MIONs – M sample has an average magnetite particle size of 120 nm while the MIONs – N sample has an average size of around 30 nm. These results strengthen previous research studies which state that the formed magnetite nanoparticles are in the nano order. In addition, these results are also reinforced by previous empirical data which state that nanoparticles are easier to form when synthesized using the down-top method [24]. Figure 4 is the result of the diffraction pattern of Magnetic Iron Oxide (MION) nanoparticles. The results of data analysis show that both samples have a cubic spinel Fe_3O_4 phase that is in accordance with the AMCSD 0000945 model data. The highest diffraction peak of the particle is observed at an angle of 2θ 35.24° with the hkl plane (311) while the distribution of other 2θ peaks is identified at angles of 18.13°, 30.25°, 43.03°, 56.97°, 63.59°, and 75.28° which correspond to the miller indices (111), (220), (222), (422), (511), (026) and (335), respectively. There is also a goethite peak (400) indicated. This is due to the presence of impurity factors caused by the calcination temperature being too low [6].

Figure 3 also observes a difference in the width of the main peaks of the two samples. This indicates a difference in size formed from the MIONs - M and MIONs N samples. The results of data analysis also show that no new phases were found in the two samples. These data indicate that the impurity of the MIONs sample is relatively small. In addition, from the diffraction peaks formed, no new peaks were found indicating that the degree of crystallinity of the MIONs is relatively high. To strengthen this analysis, the XRD data of both samples were analyzed using the refinement method and Debye Scherrer calculations and the results can be seen in Figure 4(b) and Table 2.

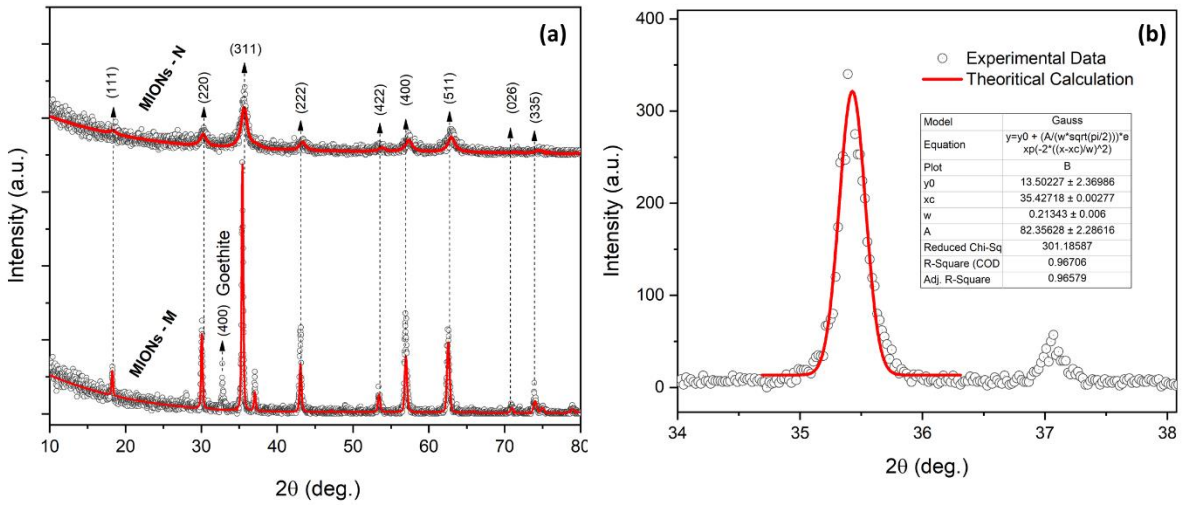

Figure 4. Diffractogram Pattern of MIONs

The results of the crystal structure analysis showed a slight difference between the lattice parameters of the MIONs - M and MIONs - N samples measured using the refinement method and the Debye-Scherrer method. Based on the refinement method, the crystal size of the Fe_3O_4 particles for the MIONs - M sample was 106.68 nm, while for the MIONs - N sample it was 9.05 nm. Meanwhile, the results of data analysis using the Debye-Scherrer method showed the crystal size of the Fe_3O_4 particles was 136.68 nm for the MIONs - M sample and 12.53 nm for the MIONs - N sample. These results indicate that the MIONs - M sample synthesized using the mechanical method is much larger compared to the MIONs - N sample using the chemical method.

Table 2. MIONs Theoretical Calculation Results Output

Parameter	M	N
Rietveld Method		
Crystallite Size (nm)	106.68	9.05
Cell Volume (Å^3)	591.64	581.35
Scale*Volume (Å^3)	0.002950	24.03 x 10^4
Molecular Weight (gr)	1852.51	1852.51
Density (gr/cm^3)	51.97	5.29
Lattice Constant (Å) (a=b=c)	8.39	8.34
Rp	16.78	15.85
Rwp	19.21	19.92
X^2	1.55	1.27
Brag-Factor	10.99	8.79
Debye-Scherrer Method		
Crystallite Size (nm)	136.68	12.53
Lattice Constant (Å) (a=b=c)	8.39	8.40

The results of this data analysis are also in accordance with previous studies, which state that the size of magnetite particles produced using the coprecipitation method gets a value at nano size [25]. These results also strengthen the statement that the down-top method is very

effective in fabricating magnetite particles on a nanometer scale. Furthermore, the different particle sizes show that MIONs - N using the modified coprecipitation method has a much smaller size than MIONs - M. In addition, the cell volume between the two samples also has a slight difference. The cell volume for the MIONs - M sample has a value of 591.64 $Å^3$ and for the MIONs - N sample it is 581.35 $Å^3$. This difference in value is the effect of the difference in crystal size of the two samples.

The molecular weight for both MIONs - M and MIONs - N samples is consistent at 1852.51 grams. This shows that the molecular weight is not affected by the synthesis method of the two samples. However, this is different from the density value of the material of the two samples. The density of the MIONs - M sample has a value of 51.97 g/cm^3 while the MIONs - N sample is in the range of 5.29 g/cm^3. This difference is due to the significant difference in crystal size between the two samples where the porosity value of the MIONs - N sample is higher than that of the MIONs - M. Referring to the lattice parameters of the data analysis results, in general the results of the MIONs - N sample data analysis are much more accurate than those of the MIONs - M sample. This can be seen from several results of the measurement lattice parameters, where the lattice parameter values of the MIONs - N sample are smaller than those of the MIONs - M. Such as the Rp (residual profile) and Rwp (weighted residual profile) values, the MIONs - M sample has values of 16.78 and 19.21 respectively, while the MIONs - N sample has values of 15.85 and 19.92 respectively. For the χ^2 number value in the MIONs - M sample is 1.55 while the MIONs - N sample is 1.27. Likewise for the Bragg factor value, the Bragg factor for the MIONs - M sample is 10.99 and the MIONs - N sample is 8.79.

VSM characterization was carried out to determine the magnetization properties of the two samples. Analysis of VSM data on both samples, namely MIONs - M and MIONs - N, obtained a magnetization hysteresis curve which can be seen in **Figure 5**.

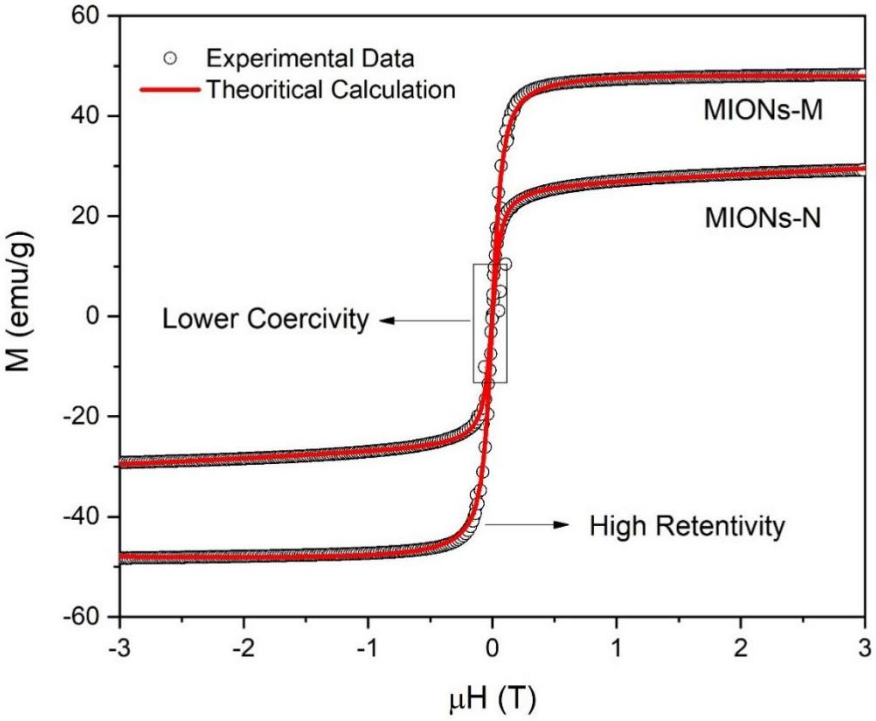

Figure 5. Hysteresis curve for MIONs - M and MIONs - N samples

Superparamagnetic materials are a type of material that only shows its magnetization response when given an external magnetic field and has no permanent magnetization or very little when the field is removed. **Figure 5** shows the results of data refinement using the Langevin equation theory calculation [26] and the magnetization values are shown in **Table 3**. Based on the results of data analysis, both samples are classified as superparamagnetic materials. This result is because the remanent magnetization and magnetic field coherence of both samples are relatively small. Theoretically, the sample magnetization equation is shown in equation (1).

$$M = M_s \left[\coth\left(\frac{\mu H}{k_b T} - \frac{k_b T}{\mu H}\right)\right] \qquad (1)$$

where M is the sample magnetization, μ is the magnetic moment, H is the magnetic field (T), kB is the Boltzman constant which has a value of 1.38 x 10^{-23} J/K and T is the room temperature (K). The magnetic parameter values are divided into several variables, namely saturation magnetization (M_s), remanent magnetization (M_r), and coercivity field (Hc). Through the magnetic data parameters above, the magnetic domain diameter (D) value can also be calculated as in equation (2).

$$D = \left(\frac{18 K_B T}{\pi} \frac{\chi_i}{\rho M_s}\right)^{\frac{1}{3}} \qquad (2)$$

where χ_i is the initial susceptibility of the sample, ρ is the particle density (obtained from the Rietica output) and Ms is the saturation magnetization (emu/g). Particle size data through equation (2) are also shown in **Table 3**.

Table 3. List of Outputs for Equation (1) and Equation (2)

Parameter	MIONs – M	MIONs – N
M_s (emu/g)	49,508 ± 0,118	26,543 ± 0,084
M_r (emu/g)	0,016 ± 0,003	0,074 ± 0,003
H_c (T)	0,031 ± 0,001	0,035 ± 0,001
χ (emu/g.T)	0,029 ± 0,006	1,074 ± 0,041
D (nm)	1,754 x 10^{-9}	1,898 x 10^{-7}
μ (J/T)	7,275 x 10^{-24}	5,025 x 10^{-19}

Table 3 shows that the M_r and H_c values of both samples are very low. It can be concluded that the MIONs - M and MIONs - N samples have characteristics as superparamagnetic materials. This result is supported by the research results reported by Karaagac and Köçkar [27], they claim that superparamagnetic particles have coercivity field values close to zero. Based on the Langevin equation, the M_s of MIONs - M sample is 49.508 ± 0.118 emu/g and the MIONs - N sample is 26.543 ± 0.084 emu/g. This magnetization shows that the MIONs - M sample has a higher magnetization capacity than the MIONs - N sample. In addition, the calculation of the magnetic moment also shows a significant difference between the two samples, the MIONs - N sample has a much larger magnetic moment (5.025 x 10^{-19} J/T) compared to the MIONs - M sample 7.275 x 10^{-24} J/T). This difference indicates that in the single domain area the smaller the particle size, the smaller the saturation magnetization value. Furthermore, through the equation used to calculate the magnetic domain diameter, it is found that the diameter of the MIONs-M magnetic domain is around 1.754 x 10^{-9} nm, while the diameter of the MIONs-N magnetic domain is around 1.898 x 10^{-7} nm. When the diameter of this magnetic domain is compared with the XRD test results, the value is relatively smaller.

The difference in value is caused by the XRD and SEM characterization using the bright-field method through the assistance of an electron beam to capture the morphology of nanoparticles so that the particle size is relatively larger while the VSM test uses the dark-field mode [24]. This phenomenon is reinforced by the findings of Anushree and Philip [28], which states that the particle size using dark-field mode such as VSM will produce a relatively smaller nano-crystalline Ni-Cu Alloy size compared to bright-field SEM mode [12]. In previous studies, iron oxide-based magnetic nanoparticles such as Fe_3O_4 have been extensively studied because of their unique properties, such as very low remanent magnetization and field coherence values so that they can be categorized as superparamagnetic materials. In addition, research by Dias et al. [29] confirmed that the M_s of superparamagnetic nanoparticles is highly dependent on particle size, with smaller particles tending to have lower Ms values.

These results are in line with the findings in this study where MIONs - N which have smaller particle sizes compared to MIONs - M have lower Ms values compared to MIONs - M. This is due to the more dominant surface effect on particles with smaller sizes. This characteristic is very important and interesting to apply in the application of several fields of nanomaterials and nanotechnology. Furthermore, research by Verma et al. [30] highlights only the potential applications of magnetic nanoparticles, particularly in biomedical fields. Specifically, the study suggests their potential for use in magnetic field-based drug delivery systems (DDS) due to the significant role of magnetic moment and particle size. However, this does not confirm direct application of the authors' research but rather indicates its prospective utility in such systems.

Conclusion

The results of the analysis of the elemental composition, morphology, and crystal structure of Magnetic Iron Oxide Nanoparticles (MIONs) show several important findings that improve our understanding of the characteristics of magnetite materials. The composition of iron (Fe) dominates the content of MIONs – M and MIONs – N samples. This indicates that MIONs – M and MIONs – N samples are pure iron-based materials that are important for magnetic applications. Titanium (Ti) is detected in the MIONs-N sample with an impurity level of 5.07% and silicon (Si), calcium (Ca) manganese (Mn) is present in both samples, which may influence their functional magnetic properties. Differences in phosphorus (P) and calcium (Ca) contents also indicate potential variations in the synthesis process or raw materials. SEM characterization reveals that MIONs particles tend to have a spherical shape and experience agglomeration.

The particle size distribution of MIONs – M has an average size of about 120 nm while MIONs – N is in the range of 30 nm. XRD data analysis shows that the Fe_3O_4 particle structure pattern has a spinel structure phase that is in accordance with the AMCSD 0000945 model data. The MIONs - M sample has a larger peak width than the MIONs - N sample so that the crystallinity size of the MIONs - M sample is larger than that of MIONs - N. Calculations using the refinement and Debye-Scherrer methods show that the crystallinity size and density of the MIONs - M sample have larger values than those of MIONs - N. Thus, the chemical synthesis method produces smaller morphology and magnetization than the mechanical method. This is important to be a reference in designing the mechanical and magnetic properties of natural iron sand-based samples for the development of nanomaterial and nanotechnology studies.

Acknowledgment

This research was funded by the Internal Fund Grant of Universitas Negeri Malang for the 2024 fiscal year through the PUI-Start Up Scheme with contract number 4.4.663/UN32.14.1/LT/2024 in the name of SN.

References

[1] H. Jia, J. Sun, M. Dong, H. Dong, H. Zhang, and X. Xie, 'Deep eutectic solvent electrolysis for preparing water-soluble magnetic iron oxide nanoparticles', *Nanoscale*, vol. 13, no. 45, pp. 19004–19011, Nov. 2021, doi: 10.1039/D1NR05813D.

[2] T. Bhardwaj and T. K. Sharma, 'Nanosensor-Enabled Microfluidic Biosensors for the Detection of Pathogenic Bacteria', in *Nanosensors for Point-of-Care Diagnostics of Pathogenic Bacteria*, A. Acharya and N. K. Singhal, Eds., Singapore: Springer Nature, 2023, pp. 85–111. doi: 10.1007/978-981-99-1218-6_5.

[3] M. M. Abutalib and A. Rajeh, 'Influence of Fe_3O_4 nanoparticles on the optical, magnetic and electrical properties of PMMA/PEO composites: combined FT-IR/DFT for electrochemical applications', Journal of Organometallic Chemistry, vol. 920, p. 121348, 2020.

[4] A. Amiri-Rigi and S. Abbasi, 'Microemulsion-based lycopene extraction: Effect of surfactants, co-surfactants and pretreatments', Food chemistry, vol. 197, pp. 1002–1007, 2016.

[5] G. Antarnusa and E. Suharyadi, 'A synthesis of polyethylene glycol (PEG)-coated magnetite Fe_3O_4 nanoparticles and their characteristics for enhancement of biosensor', Mater. Res. Express, vol. 7, no. 5, p. 056103, May 2020, doi: 10.1088/2053-1591/ab8bef.

[6] A. Taufiq et al., 'Synthesis of magnetite/silica nanocomposites from natural sand to create a drug delivery vehicle', Heliyon, vol. 6, no. 4, Apr. 2020, doi: 10.1016/j.heliyon.2020.e03784.

[7] Y. A. Hariyanto, A. Taufiq, and S. Soontaranon, 'Investigation on the three-dimensional nanostructure and the optical properties of hydroxyapatite/magnetite nanocomposites prepared from natural resources', Journal of the Korean Physical Society, vol. 75, pp. 708–715, 2019.

[8] S. Sunaryono, M. F. Hidayat, N. Mufti, S. Soontaranon, and A. Taufiq, 'The effect of Mn doping on nano structure and magnetic properties of $Mn_xFe_{3-x}O_4$-PEG/PVP/PVA based ferrogel', J Polym Res, vol. 27, no. 9, p. 284, Aug. 2020, doi: 10.1007/s10965-020-02065-w.

[9] S. Sunaryono et al., 'Investigating the specific absorption rate and antimicrobial activity of $Mn_{0.25}Fe_{2.75}O_4$/Ag ferrogel based on carboxymethyl cellulose/polyvinyl alcohol composite polymer', Journal of Thermoplastic Composite Materials, p. 08927057231167419, Mar. 2023, doi: 10.1177/08927057231167419.

[10] C.-H. Huang, T.-J. Chuang, C.-J. Ke, and C.-H. Yao, 'Doxorubicin–Gelatin/Fe_3O_4–Alginate Dual-Layer Magnetic Nanoparticles as Targeted Anticancer Drug Delivery Vehicles', Polymers, vol. 12, no. 8, Art. no. 8, Aug. 2020, doi: 10.3390/polym12081747.

[11] M. Chang et al., 'Two-dimensional interface engineering of NiS/MoS2/Ti3C2Tx heterostructures for promoting electromagnetic wave absorption capability', Composites Part B: Engineering, vol. 225, p. 109306, Nov. 2021, doi: 10.1016/j.compositesb.2021.109306.

[12] D. M. Fernandes et al., 'Novel electrochemical sensor based on N-doped carbon nanotubes and Fe3O4 nanoparticles: Simultaneous voltammetric determination of ascorbic acid, dopamine and uric acid', Journal of Colloid and Interface Science, vol. 432, pp. 207–213, Oct. 2014, doi: 10.1016/j.jcis.2014.06.050.

[13] B. L. Pathirannahel, Development of Microfluidic Paper Based Analytical Devices (Pads) for the Detection of Calcium and Magnesium Ions. Western Carolina University, 2018.

[14] A. Taufiq et al., 'Investigation of structural, magnetic and antibacterial activities of $Cr_xFe_{3-x}O_4$ ferrofluids', Molecular Crystals and Liquid Crystals, vol. 694, no. 1, pp. 60–72, 2019.

[15] N. P. D. Kristina, I. G. Arjana, and P. Yasa, 'Synthesis and Characterization Of Magnetite Nanomaterials In Tianyar Iron Sand Using Co-Precipitation Method', Indonesian Physical Review, vol. 7, no. 3, pp. 398–413, Jul. 2024, doi: 10.29303/ipr.v7i3.328.

[16] M. K. Ahmed, A. A. Menazea, S. F. Mansour, and R. Al-Wafi, 'Differentiation between cellulose acetate and polyvinyl alcohol nanofibrous scaffolds containing magnetite nanoparticles/graphene oxide via pulsed laser ablation technique for tissue engineering applications', Journal of Materials Research and Technology, vol. 9, no. 5, pp. 11629–11640, 2020.

[17] A. Taufiq *et al.*, 'Effects of the Annealing Temperature on the Structure Evolution and Antifungal Performance of TiO_2/Fe_3O_4 Nanocomposites Manufactured from Natural Sand', *Nano*, vol. 16, no. 02, p. 2150017, 2021.

[18] K. W. Mas' udah, P. E. Yuwita, Y. A. Haryanto, A. Taufiq, and Sunaryono, 'Effect of heat treatment on carbon characteristic from corncob powders prepared by coprecipitation method', in *AIP Conference Proceedings*, AIP Publishing LLC, 2020, p. 040044.

[19] Maulinda, I. Zein, and Z. Jalil, 'Identification of Magnetite Material (Fe_3O_4) Based on Natural Materials as Catalyst for Industrial Raw Material Application', *J. Phys.: Conf. Ser.*, vol. 1232, no. 1, p. 012054, Sep. 2019, doi: 10.1088/1742-6596/1232/1/012054.

[20] Z. Jalil, E. N. Sari, I. Ismail, Muhammad, M. N. Machmud, and E. Handoko, 'Natural magnetite characterization from beach sand prepared by using planetary ball milling', J. Phys.: Conf. Ser., vol. 1825, no. 1, p. 012070, Feb. 2021, doi: 10.1088/1742-6596/1825/1/012070.

[21] R. B. Istiningrum, F. L. U. Pamungkas, S. J. Santosa, and Nuryono, 'Ultrasound-assisted extraction of magnetic material from natural iron sand', *AIP Conference Proceedings*, vol. 2296, no. 1, p. 020072, Nov. 2020, doi: 10.1063/5.0030725.

[22] K. Saputra, S. Sunaryono, S. Hidayat, H. Wisodo, and A. Taufiq, 'Investigation of nanostructural and magnetic properties of Mn0.25Fe2.75O4/AC nanoparticles', *Materials Today: Proceedings*, vol. 44, pp. 3350–3354, Jan. 2021, doi: 10.1016/j.matpr.2020.11.646.

[23] M. Bobik, I. Korus, K. Synoradzki, J. Wojnarowicz, D. Biniaś, and W. Biniaś, 'Poly (sodium acrylate)-modified magnetite nanoparticles for separation of heavy metals from aqueous solutions', *Materials*, vol. 15, no. 19, p. 6562, 2022.

[24] R. E. Saputro, A. Taufiq, Sunaryono, N. Hidayat, and A. Hidayat, 'Effects of DMSO content on the optical properties, liquid stability, and antimicrobial activity of Fe_3O_4/OA/DMSO ferrofluids', *Nano*, vol. 15, no. 05, p. 2050067, 2020.

[25] M. F. Hidayat, N. Mufti, and E. Latifah, 'Study on distribution of magnetite ($Fe_{3-x}Mn_xO_4$) filler in $Fe_{3-x}Mn_xO_4$-PEG/PVA/PVP magnetic hydrogel by using twolognormal function analysis', in *IOP Conference Series: Materials Science and Engineering*, IOP Publishing, 2019, p. 012024.

[26] H. Vroylandt, 'On the derivation of the generalized Langevin equation and the fluctuation-dissipation theorem', *EPL*, vol. 140, no. 6, p. 62003, Dec. 2022, doi: 10.1209/0295-5075/acab7d.

[27] O. Karaagac and H. Köçkar, 'Improvement of the saturation magnetization of PEG coated superparamagnetic iron oxide nanoparticles', *Journal of Magnetism and Magnetic Materials*, vol. 551, p. 169140, Jun. 2022, doi: 10.1016/j.jmmm.2022.169140.

[28] C. Anushree and J. Philip, 'Efficient removal of methylene blue dye using cellulose capped Fe_3O_4 nanofluids prepared using oxidation-precipitation method', *Colloids and Surfaces A: Physicochemical and Engineering Aspects*, vol. 567, pp. 193–204, 2019.

[29] A. M. M. Dias *et al.*, 'Superparamagnetic Iron Oxide Nanoparticles for Immunotherapy of Cancers through Macrophages and Magnetic Hyperthermia', *Pharmaceutics*, vol. 14, no. 11, Art. no. 11, Nov. 2022, doi: 10.3390/pharmaceutics14112388.

[30] C. Verma, D. K. Verma, E. Berdimurodov, I. Barsoum, A. Alfantazi, and C. M. Hussain, 'Green magnetic nanoparticles: a comprehensive review of recent

progress in biomedical and environmental applications', *J Mater Sci*, vol. 59, no. 2, pp. 325–358, Jan. 2024, doi: 10.1007/s10853-023-08914-5.